Title
A STATISTICAL MODEL OF BRITTLE FRACTURE BY TRANSGRANULAR CLEAVAGE

Authors
Lin, T.
Evans, A.G.
Ritchie, R.O.

Publication Date
1985-05-01

Lawrence Berkeley Laboratory
UNIVERSITY OF CALIFORNIA

Materials & Molecular Research Division

Submitted to Journal of Mechanics and Physics of Solids

A STATISTICAL MODEL OF BRITTLE FRACTURE BY TRANSGRANULAR CLEAVAGE

T. Lin, A.G. Evans, and R.O. Ritchie

May 1985

Prepared for the U.S. Department of Energy under Contract DE-AC03-76SF00098

DISCLAIMER

LBL-19673

A STATISTICAL MODEL OF BRITTLE FRACTURE BY TRANSGRANULAR CLEAVAGE

by

Tsann Lin, A. G. Evans, and R. O. Ritchie

Materials and Molecular Research Division
Lawrence Berkeley Laboratory
and
Department of Materials Science and Mineral Engineering
University of California, Berkeley, CA 94720

May 1985

submitted to

Journal of Mechanics and Physics of Solids

This work was supported by the Director, Office of Energy Research, Office of Basic Energy Sciences, Materials Science Division of the U.S. Department of Energy under Contract No. DE-AC03-76SF00098.

A STATISTICAL MODEL OF BRITTLE FRACTURE BY TRANSGRANULAR CLEAVAGE

Tsann Lin, A. G. Evans, and R. O. Ritchie

Materials and Molecular Research Division,
Lawrence Berkeley Laboratory, and
Department of Materials Science and Mineral Engineering,
University of California, Berkeley, California

SUMMARY

A model for brittle fracture by transgranular cleavage cracking is presented based on the application of weakest link statistics to the critical microstructural fracture mechanisms. The model permits prediction of the macroscopic fracture toughness, K_{Ic}, in single phase microstructures containing a known distribution of particles, and defines the critical distance from the crack tip at which the initial cracking event is most probable. The model is developed for unstable fracture ahead of a sharp crack considering both linear elastic and nonlinear elastic ("elastic/plastic") crack tip stress fields. Predictions are evaluated by comparision with experimental results on the low temperature flow and fracture behavior of a low carbon mild steel with a simple ferrite/grain boundary carbide microstructure.

NOTATION

δA	elemental area within active zone
b	characteristic dimension along crack front
c_o	diameter of cracked particle
d_g	average grain diameter
E	Young's modulus
f	"eligibility" factor in Eq. (4)
F	dimensionless parameter defining $(\sigma_{ij}/\sigma_o)_{max}$
$g(S)dS$	elemental strength distribution of particles
h_{ij}	dimensionless function of Θ
I_n	dimensionless parameter in HRR singular solution Eq. (6)
J	amplitude of HRR singular solution of crack tip field
K_I	stress intensity factor (Mode I)
K_{Ic}	plane strain fracture toughness
l_o^*	characteristic distance (along $\Theta = 0$)
m	shape factor in Weibull assumption
n	work hardening exponent $(1 < n < \infty)$
N	number of particles per unit volume
r, Θ	polar coordinates, centered at crack tip
r_u	distance from tip where $\sigma = S_u$
r^*	distance from tip where $d\delta\varphi = 0$
r_f^*	radial characteristic distance from tip (at $K_I = K_{Ic}$)
r_y	plastic zone size
S	fracture strength of particle

S_m	strength parameter
S_o, S_u	Weibull parameters
δV, V	elemental and total active zone volume, respectively
x	distance directly ahead of crack tip
X	ratio S/S_u
α	material constant in constitutive law Eq. (5)
γ_p	"effective" fracture surface energy
δ	crack tip opening displacement
ξ	function defined in Eq. (11)
η	function defined in Eq. (16)
ν	Poisson's ratio
σ	local stress within plastic zone
σ^*	local stress when $d\delta\varphi = 0$
$\bar{\sigma}$, $\bar{\epsilon}$	equivalent stress and strain, respectively
σ_1	maximum principal stress
σ_f^*	cleavage fracture stress (at $K_I = K_{Ic}$)
σ_{ij}	stress tensor for local crack tip stresses
$\tilde{\sigma}_{ij}$	function in HRR singular solution Eq. (6)
σ_o, ϵ_o	yield (or flow) stress and strain, respectively
σ_{yy}	local tensile stress
$\sigma_{\Theta\Theta}$	local tangential stress
$\delta\varphi$, Φ	elemental and total failure probabilities, respectively

I. INTRODUCTION

Low strength structural steels fail by catastrophic brittle fracture at low temperatures. Such failures can be either transgranular or intergranular. In most ferritic steels, however, fracture occurs by transgranular cleavage cracking along well-defined, low index crystallographic planes (e.g., HAHN, AVERBACH, OWEN and COHEN, 1959; KNOTT, 1973; HAHN, 1984). The process of cleavage fracture has been attributed primarily to slip-induced cracking of carbide particles,[1] generally located on grain boundaries, followed by propagation of the resultant cracks into the surrounding ferrite matrix (Fig. 1) (McMAHON and COHEN, 1965). The critical step in this process is typically the propagation of the carbide microcrack into the adjoining ferrite grain (SMITH, 1966), except either at temperatures close to the transition temperature or in fine-grained microstructures, whereupon the critical step may become the propagation of the cleavage crack across the next grain boundary (MAN and HOLZMANN, 1971; GROOM and KNOTT, 1975).

Cleavage fracture ahead of a rounded notch (with root radius large compared to microstructural dimensions) has been considered to occur when the maximum value of the local tensile stress exceeds a

---

[1] At very low temperatures in mild steels and in higher Mn-containing steels, cleavage may be nucleated by twinning rather than slip (KNOTT and COTTRELL, 1963; OATES, 1969). Moreover, evidence of cleavage nucleation at manganese sulphide inclusions has been reported in higher strength bainitic steels (ROSENFIELD, SHETTY, and SKIDMORE, 1983).

critical fracture stress, generally regarded as a temperature and strain rate insensitive quantity (KNOTT, 1966; WILSHAW, RAU, and TETELMAN, 1968). The maximum stress occurs close to the plastic-elastic interface, at least when plasticity is confined to the notch root (i.e., for loads well below general yield) (HILL, 1950; GRIFFITHS and OWEN, 1971). Consequently, the initial cracking event occurs at a distance ahead of the crack tip of the order of the plastic zone size. Conversely, for cleavage fracture ahead of a microscopically-sharp crack, the maximum stress for contained yielding occurs within two crack tip opening displacements of the crack tip (RICE and JOHNSON, 1970). Hence, RITCHIE, KNOTT and RICE (1973) postulated that the local tensile stress must exceed the fracture stress **over a microstructurally-significant (characteristic) distance ahead of the crack tip** (Fig. 2). In their original model (hereafter referred to as RKR), the characteristic distance (for a coarse-grained high-nitrogen mild steel) was found to be a small multiple of the average ferrite grain diameter. Subsequent studies, however, have shown that the critical distance can become independent of grain size at small grain sizes (CURRY and KNOTT, 1976).

To relate the RKR criterion to the microstructural features of cleavage fracture, CURRY and KNOTT (1978) postulated that fracture initiates from the largest observable carbide, i.e., the carbide having the lowest "strength". This assumption is deemed reasonable when the stress is almost uniform, as in the case of fracture ahead

of a rounded notch. However, for fracture ahead of a sharp crack, where the stress gradient is substantial, the more numerous finer carbides also may participate in the cleavage process.

In order to examine this competition between cracked carbides of different sizes within the stress field of a sharp crack, CURRY and KNOTT (1979), and subsequently others (EVANS, 1983; BEREMIN, 1983; WALLIN, SAARIO, and TÖRRÖNEN, 1984), have re-formulated the RKR model on the basis of weakest link statistics. For this purpose, the pre-existence of a distribution of cracked carbides, each with a "strength" S inversely related to its size, is postulated. The cleavage fracture toughness then is estimated by sampling the plastic zone for the presence of an "eligible" particle at which the fracture criterion can be satisfied.

In the present study, a fully quantitative weakest link model for cleavage fracture is presented. The approach differs from previous analyses, primarily in the choice of active zone elements consistent with crack tip stress distributions. The model is used to ascribe consistent microstructural significance to the characteristic distance, and principally to predict the lower shelf plane strain fracture toughness, K_{Ic}, as a function of temperature and microstructure. Predictions are evaluated on the basis of experimental low temperature flow and fracture results in spheroidized AISI 1008 mild steel.

II. THE STATISTICAL MODELS

1. General Principles

In the present model, particles located within the plastic zone are considered to exhibit cracking and the resultant cracks are treated as non-interacting flaws capable of propagating unstably into the surrounding matrix. Weakest link statistics thus are deemed applicable. The propagation of a particle microcrack into the matrix is assumed to occur at a critical stress, characteristic of the carbide "strength" S. For a spheroidal particle containing a penny-shaped crack, S is related to the particle diameter, c_o, as (CURRY and KNOTT, 1978):

$$S^2 = \pi E \gamma_p/(1 - \nu^2)\, c_o \qquad \ldots.(1)$$

where γ_p is the effective fracture surface energy of the matrix, E is Young's modulus and ν is Poisson's ratio. The size distribution of the particles thus can be associated directly with a strength distribution, g(S)dS - the number of cracked particles per unit volume having strengths between S and S+dS. Weakest link statistics then require that elements δV within the plastic zone, subject to a stress σ, have the failure probability, $\delta\varphi$ (MATTHEWS, SHACK, and McCLINTOCK, 1976):

$$\delta\varphi = 1 - \exp\left[-\,\delta V \int_o^{\sigma} g(S)dS\right] , \qquad \ldots.(2)$$

and that the total failure probability Φ (due to the unstable propagation of the crack in the weakest particle), be given by:

$$\Phi = 1 - \exp\{-\int_0^V [dV \int_0^\sigma g(S)dS]\} \quad , \qquad \ldots.(3)$$

where V is the plastic zone volume. A convenient and versatile expression for g(S)dS is the three-parameter WEIBULL (1939) assumption:

$$\int_0^\sigma g(S)dS = \left(\frac{\sigma - S_u}{S_o}\right)^m fN \quad , \qquad \ldots.(4)$$

where m is a shape factor, S_o is a scale parameter, S_u is a lower bound strength (of the largest feasible cracked particle), and N is the number of particles per unit volume. The parameter f represents the fraction of "eligible" particles that participate in the fracture process, as dicated by the location of the particle, the orientation of the matrix grain, and so forth.

Given the stress distribution within the plastic zone, the survival probability of the structure may be ascertained from Eq. (3) by separately assessing S_o, S_u, N and m from quantitative measurements of the particle size distribution, and by independently evaluating f. Solutions to this problem for extension of a sharp crack are developed below.

2. Extension of a Sharp Crack

Crack Tip Stress Fields: For conditions of small-scale yielding in a power hardening (incompressible nonlinear elastic) solid that satisfies the constitutive law:

$$\bar{\varepsilon}/\varepsilon_o = \alpha(\bar{\sigma}/\sigma_o)^n \quad , \qquad \ldots.(5)$$

the stress field at distance r ahead of a stationary crack, in the limit of $r \to 0$, is given by the HRR singular solution (HUTCHINSON, 1968; RICE and ROSENGREN, 1968):

$$\frac{\sigma_{ij}}{\sigma_o} \to \left(\frac{J}{\alpha\, \varepsilon_o\, \sigma_o\, I_n\, r}\right)^{\frac{1}{(n+1)}} \tilde{\sigma}_{ij}(n,\theta) \quad , \qquad \ldots.(6)$$

where σ_o and ε_o are the yield strength and yield strain, respectively, α is a material constant of order unity, n is the work hardening exponent, J is the path independent integral (RICE, 1967) and I_n and $\tilde{\sigma}_{ij}$ are dimensionless parameters (SHIH, 1983). By re-expressing Eq. (6) in terms of the Mode I stress intensity factor, K_I, and by noting that the stresses predicted by the HRR solution are truncated directly by crack tip blunting (RICE and JOHNSON, 1970; McMEEKING, 1977), the plane strain stress field within the near tip region has the characteristics:

$$\frac{\sigma_{ij}}{\sigma_o} = \left[\left(\frac{1-\nu^2}{I_n}\right)\left(\frac{K_I}{\sigma_o\sqrt{r}}\right)^2\right]^{\frac{1}{(n+1)}} \tilde{\sigma}_{ij}(n,\theta) \quad , \quad (2\delta \lesssim r \lesssim 10\delta)$$

$$\frac{\sigma_{ij}}{\sigma_o} \approx F(n) \quad , \qquad (r \lesssim 2\delta) \qquad \ldots.(7)$$

where δ is the crack tip opening displacement and F(n) is a dimensionless parameter describing the maximum stress intensification at the tip, defined by the blunting solutions (Fig. 4a). Further from the crack tip (i.e., typically at $r \gtrsim 10\delta$), the stresses within the plastic zone deviate from the asymptotic HRR solution (OSTERGREN, 1969; TRACEY, 1976), such that close to the elastic-plastic interface, the solutions closely approximate the linear elastic asymptotic solution (WILLIAMS, 1957):

$$\sigma_{ij} \rightarrow \frac{K_I}{\sqrt{2\pi r}} h_{ij}(\Theta) \quad , \qquad (r \gtrsim 100\delta) \quad ....(8)$$

as shown in Fig. 4b.

At low temperatures, because the plastic zone is small, the site of the most probable cracking event is close to the elastic-plastic interface. In contrast, at higher temperatures, the most probable site resides well within the plastic zone, due to the associated increase in plastic zone size. Accordingly, the statistical analysis is performed using the two limiting idealizations for the crack tip stress distributions.[2] Behavior at the lowest temperatures (i.e., at highest σ_0) is described using the far-field linear elastic solution (Eq. (8)), resulting in an asymptotic lower bound estimate of K_{Ic}.

---

[2]Incorporation of the more precise numerical solutions of OSTERGREN (1969) and TRACEY (1976) for the description of the far-field crack tip stresses was not possible in the present model as such solutions are available only for the σ_{yy} tensile opening stresses and not the complete stress tensor σ_{ij}.

At higher temperatures closer to the transition temperature, behavior is described in terms of the near-tip HRR solution (Eq. (6)), with stresses truncated at $r \sim 2\delta$ by crack tip blunting. Intermediate temperature behavior can be ascertained by interpolation. The method of analysis is presented in its entirety for the latter case, involving the HRR formulation. Only final solutions are provided for the elastic analysis.

Statistical Analysis: The statistical analysis based on the crack tip stress fields can be performed most conveniently by defining active elements (Fig. 3). These represent elements in which the stress is constant, i.e., in which particle microcracks liable to be activated all have strengths less than, or equal to, the appropriate local stress σ. Such elements have a volume δV given by:

$$\delta V = 2b \int_0^{\pi} r \, \delta r \, d\Theta \quad , \qquad \ldots.(9)$$

where b is a characteristic dimension along the crack front (EVANS, 1983), the element location is defined by:

$$r = \left(\frac{K_I}{\sigma_o}\right)^2 \left(\frac{1 - \nu^2}{I_n}\right)\left(\frac{\sigma_o}{\sigma}\right)^{n+1} \tilde{\sigma}^{n+1} \quad , \qquad \ldots.(10)$$

and σ is the stress component that allows linkage of activated microcracks with the main crack tip. The failure probability associated with such elements is then:

$$\delta\varphi = 1 - \exp[-\, bfN\, \xi\, K_I^4\, \sigma_o^{2(n-1)} (\sigma - S_u)^m\, \sigma^{-(2n+3)}\, S_o^{-m}\, d\sigma] \quad ,$$

with

$$\xi = 2(n+1)\left[\frac{1 - \nu^2}{I_n}\right]^2 \int_o^{\pi} \tilde{\sigma}^{2(n+1)}\, d\theta \quad . \qquad \ldots.(11)$$

The model is evaluated for σ representing either the principal tensile stress, σ_1, or the tangential stress, $\sigma_{\theta\theta}$ (Fig. 3). These assumptions regarding σ are tantamount to presuming, respectively, that all activated particle microcracks link with the crack tip or, that only those microcracks radially oriented with respect to the main crack tip are amenable to linkage.

The elemental survival probability expressed by Eq. (11) exhibits a minimum at a characteristic distance r^* from the crack tip, given by ($d\delta\varphi = 0$):

$$r^* = \left[\frac{1 - \nu^2}{I_n}\right]\left[\frac{2n + 3 - m}{2n + 3}\right]^{n+1}\left(\frac{K_I}{\sigma_o}\right)^2\left(\frac{\sigma_o}{S_u}\right)^{n+1} \tilde{\sigma}^{n+1} \quad , \quad \ldots.(12)$$

occurring at the stress:

$$\sigma^* = \left[\frac{2n + 3}{2n + 3 - m}\right] S_u \quad , \qquad \ldots.(13)$$

as illustrated schematically in Fig. 5. When cleavage fracture occurs at $K_I = K_{Ic}$, the critical values of σ^* and r^*, σ_f^* and r_f^*, respectively, can be equated conceptually with the critical fracture

stress and characteristic distance invoked in the RKR analysis. In statistical terms, the distance r^* represents the location ahead of the crack tip where the initial cracking event is most probable. Since, for a sharp crack, the local stresses are progressively decreased over microstructurally-significant dimensions ahead of the crack tip, the value of r^* reflects the competition between behavior far from the tip, where the population of eligible cracked particles is large but the stresses are low, and behavior close to the tip, where the stresses are higher but the number of eligible particles is less.

The total survival probability of material within the plastic zone can be obtained from the product of the elemental survival probabilities:

$$\Phi = 1 - \exp\left[- bfN \xi K_I^4 \sigma_o^{2(n-1)} S_o^{-m} \int_{S_m}^{\sigma_o F} \sigma^{-(2n+3)} (\sigma - S_u)^m \, d\sigma \right] \quad , (14)$$

where S_m is the larger amongst S_u and σ_o. Consequently, at the median level ($\Phi = 1/2$) where $K_I = K_{Ic}$, the fracture toughness becomes:

$$K_{Ic} = \left[\frac{\ell n\, 2}{fNb\xi\eta}\right]^{\frac{1}{4}} \left(\frac{S_o}{S_u}\right)^{m/4} S_u^{(1+n)/2} \sigma_o^{(1-n)/2} \quad , \qquad \ldots.(15)$$

where for the case of present interest ($S_u > \sigma_o$),[3]

---

[3]The weakest carbide always has a strength in excess of the yield strength for the material, AISI 1008 mild steel, studied in section III.

$$\eta(m,n,S_u/\sigma_o) = \int_1^{F\sigma_o/S_u} (X - 1)^m X^{-(2n+3)}\, dX \quad , \qquad ....(16)$$

where $X = S/S_u$.

Corresponding solutions for r^* and σ^* based on far-field, linear elastic stress distributions are given below:

$$r^* = \frac{(5 - m)^2}{50\pi} \left(\frac{K_I}{S_u}\right)^2 \quad , \qquad ....(17)$$

$$\sigma^* = \left[\frac{5}{5 - m}\right] S_u \quad , \qquad ....(18)$$

such that the fracture toughness becomes:

$$K_{Ic} = \left[\frac{\ell n\ 2}{fNb\eta\ 1.35}\right]^{\frac{1}{4}} \left(\frac{S_o}{S_u}\right)^{m/4} S_u \quad . \qquad ....(19)$$

Some specific trends in toughness predicted by Eqs. (15) and (19) are plotted in Fig. 6. The linear elastic solution evidently provides a temperature-independent K_{Ic} asymptote at low temperatures, while the near-tip HRR solution results in K_{Ic} values asymptotic to a transition temperature (which occurs when the integration limits in Eq. (14) converge). Additionally, comparision of the expression for the local fracture stress, σ_f^*, evaluated from the HRR formulation (Eq. (13)), with that from the far-field formulation (Eq. (18)), reveals that σ_f^* is predicted to be weakly dependent on temperature.

III. EXPERIMENTAL PROCEDURES

The material used to evaluate the model was an AISI 1008 mild steel of composition shown in Table I:

Table I: Composition in wt.% of AISI 1008 steel

C	Mn	P	S	Si	Fe
0.08	0.26	0.01	0.01	0.01	balance

To obtain a microstructure consisting of a ferritic matrix with primarily grain boundary carbides, the steel was austenitized for 1 hr at 920°C, air cooled, and then spheroidized for 7 days at 700°C. The resulting microstructure, termed L7, was found to have an average ferrite grain size (d_g) of 25 μm and a grain boundary carbide particle size distribution shown by the histogram in Fig. 7. Using this size distribution, the elemental strength distribution g(S)dS, was derived directly using Eq. (1). Values of the Weibull parameters m, S_o and S_u, computed from g(S)dS assuming Eq. (4), are listed in Table II.

Table II: Grain size and grain boundary carbide strength distribution

Structure	Ferrite Grain Size	Carbide Strength Distribution		
	d_g (μm)	m	S_o (MPa)	S_u (MPa)
L7	25	1.7	2800	1300

Mechanical properties were assessed from uniaxial tensile tests conducted at a displacement rate of 0.5 mm/min over the temperature range -196°C to 20°C. Results showing the temperature dependence of strength and ductility are plotted in Fig. 8. Work hardening exponents were found to be approximately 4 below -70°C. Plane strain fracture toughness tests to measure K_{Ic} values were performed on fatigue pre-cracked single-edge-notched bend specimens, tested in four-point bend over the temperature range -196°C to -70°C, in accordance primarily with ASTM Standard E-399. At the higher temperatures where excessive plasticity invalidated direct linear elastic measurements of toughness, values of K_{Ic} were computed from nonlinear elastic J_{Ic} measurements, i.e., $J_{Ic} = K_{Ic}^2/E$, using the experimental procedures of SUMPTER and TURNER (1976). Resulting plane strain fracture toughness data are shown in Fig. 9.

IV. COMPARISON BETWEEN THEORY AND EXPERIMENT

Model predictions for the fracture toughness K_{Ic} of AISI 1008 steel as a function of temperature are shown in Fig. 10 and are compared to the experimental results of Fig. 9. Predictions are based on a maximum principal stress criterion, with the fraction f of "eligible" carbides set at 5%. A value of 23 J/m^2 is assumed for the effective fracture surface energy γ_p (GERBERICH and KURMAN, 1985). The characteristic crack front width, b, is assessed from the

particle activation probability along the crack front (LIN, EVANS, and RITCHIE, 1985) and is taken to be $2d_g$.

It is apparent that the predicted asymptotic lower shelf toughness is consistent with the minimal variation in toughness observed at the lowest temperatures. At higher temperatures, predictions using the nonlinear elastic HRR distribution (plotted for work hardening exponents, n, between 3 and 5) yield sharply increasing toughness values, consistent with transitional behavior approaching the upper shelf. As n is approximately 4 for this microstructure, the absolute magnitude of the cleavage fracture toughness predictions can be seen to agree closely with experimental K_{Ic} values for this steel.

Observations of a lower shelf fracture toughness independent of yield strength, even though the yield stress is changing rapidly, have been noted previously (e.g., LUCAS and ODETTE, 1984; RITCHIE, SERVER and WULLAERT, 1979), and reflect initial fracture events dominated primarily by far-field near-elastic stresses, due to the small plastic zone size. With increasing temperature, the corresponding plastic zone size increases, such that fracture events become dominated by the near-tip elastic-plastic stresses, resulting in a toughness that depends on the yield strength and that increases with increasing temperature. The asymptotic transition temperature is the temperature at which the yield strength is reduced to an extent that the maximum crack tip stress, determined by the blunting

solution (Fig. 4b), becomes insufficient to exceed the minimum carbide strength S_u.

The model permits investigation into the orientation and eligibility of carbide particle cracks in the fracture process. Predictions based on a critical value of the tangential stress, $\sigma_{\theta\theta}$, rather than σ_1, yield unreasonably high values of the toughness (Fig. 11). This trend is consistent with metallographic studies (LIN, EVANS, and RITCHIE, 1985), which indicate that linkage with the macrocrack tip is not restricted to radially-oriented particle cracks. Furthermore, for the present microstructure, it appears that the data require roughly 5% of the carbide population to be eligible as fracture sites (Fig. 12), again consistent with metallographic studies of the crack tip region. In fact, the fraction of eligible carbides probably decreases at the higher temperatures, in the transition range, because metallographic studies show that numerous particle cracks become blunted and play no further active role in the fracture process (see also COHEN and VUKCEVICH, 1969). This "exhaustion" behavior results in a more rapid approach to the transition than predicted by Figs. 6, 10-12. Details of the microstructural implications of this model, specifically with respect to the question of the "exhaustion" of particle cracks and the independent roles of grain size and particle size, are treated in detail elsewhere (LIN, EVANS and RITCHIE, 1985).

VI. DISCUSSION

The statistical model for transgranular cleavage fracture described above, which permits prediction of the cleavage fracture toughness for a microstructure containing a known distribution of particles, is seen to provide excellent agreement with experimental K_{IC} results in a mild steel. However, there are several limitations with the approach which should be noted.

First, the model presumes a criterion for fracture wherein the critical event is the propagation into the matrix of a microcrack within a carbide particle. The majority of experimental evidence, on low temperature cleavage cracking in steels, supports such a notion (e.g., KNOTT, 1973; HAHN, 1984). However, should the critical event change to the propagation of a ferrite microcrack through the grain boundary, as has been inferred by certain authors for temperatures closer to the transition (e.g., MAN and HOLZMANN, 1971), a weakest link model is unlikely to be appropriate as the rate-limiting step probably will involve the coalescence of such cracks for unstable fracture.

Second, the question of the fraction of eligible particle microcracks involved in the fracture process currently is not amenable to prediction, especially when "exhaustion" of certain particle cracks occurs at higher temperatures. Orientation and location clearly are relevant here. In this context, the current

analysis indicates that the critical fracture event is not restricted solely to radially orientated microcracks.

Finally, the current model relies on the asymptotic linear elastic and HRR nonlinear elastic singular solutions to describe the distribution of stresses in the vicinity of the crack tip. Whereas these solutions provide reasonable limiting descriptions of the local stresses at the elastic/plastic interface and near the crack tip, respectively (Fig. 4), a more accurate representation would be obtained with the numerical power hardening solutions of TRACEY (1976) and McMEEKING (1977). However, as noted above, the latter solutions are available for the σ_{yy} stresses only, and thus are difficult to incorporate with the active zone concept implicit in the current model.

VII. CONCLUSIONS

A model for transgranular cleavage fracture relying on weakest link statistical considerations has been presented for the prediction of brittle fracture toughness in single phase microstructures containing a known distribution of particle microcracks. The model, which considers cracking events within an active zone defined in terms of either the nonlinear elastic near-tip or linear elastic far-field crack tip stress fields, permits prediction of the temperature dependence of K_{IC}, as a function of such variables as flow stress, work hardening exponent and particle size, from lower shelf

temperatures into the ductile/brittle transition region. The analysis provides a natural definition of the "characteristic distance" as the critical radial dimension from the crack tip where the initial cracking event is most probable. In comparison with experiment, model predictions are found to agree closely with plane strain fracture toughness results measured in a low strength mild steel over a range of temperatures.

ACKNOWLEDGMENTS

This work was supported by the Director, Office of Energy Research, Office of Basic Energy Sciences, Materials Science Division of the U.S. Department of Energy under Contract No. DE-AC03-76SF00098. The writers wish to thank Profs. R. M. McMeeking and G. R. Odette for several helpful discussions.

REFERENCES

BEREMIN, F.M. 1983 Metall. Trans. A **14A**, 2277.

COHEN, M. and VUKCEVICH, M.R. 1969 Physics of Strength and Plasticity (ed. Argon, A.S.), p. 295, M.I.T. Press, MA.

CURRY, D. and KNOTT, J.F. 1976 Met. Sci. **10**, 1.

CURRY, D. and KNOTT, J.F. 1978 Ibid. **12**, 511.

CURRY, D. and KNOTT, J.F. 1979 Ibid. **13**, 341.

EVANS, A.G. 1983 Metall. Trans. A **14A**, 1349.

GERBERICH, W.W. and KURMAN, E. 1985 Scripta Met. **19**, 295.

GRIFFITHS, J.R. and OWEN, D.R.J. 1971 J. Mech. Phys. Solids **19**, 419.

GROOM, J.D.G. and KNOTT, J.F. 1975 Met. Sci. **9**, 390.

HAHN, G.T. 1984 Metall. Trans. A **15A**, 947.

HAHN, G.T., AVERBACH, B.L., OWEN, W.S. and COHEN, M. 1959 Fracture (ed. Averbach, B.L. et al.), p. 91, Wiley, N.Y.

HILL, R. 1950 The Mathematical Theory of Plasticity, Oxford Univ. Press.

HOLZMANN, M. and MAN, J. 1971 J. Iron Steel Inst. **209**, 836.

HUTCHINSON, J.W. 1968 J. Mech. Phys. Solids **16**, 13.

KNOTT, J.F. 1966 J. Iron Steel Inst. **204**, 104.

KNOTT, J.F. 1973 Fundamentals of Fracture Mechanics, Butterworths, London.

KNOTT, J.F. and COTTRELL, A.H. 1963 J. Iron Steel Inst. **201**, 249.

LIN, T., EVANS, A.G. and RITCHIE, R.O. 1985 Metall. Trans. A **16A**, in review.

MATTHEWS, J.R., SHACK, W. and McCLINTOCK, F.A. 1976 J. Amer. Ceram. Soc. **59**, 304.

McMAHON, C.J. and COHEN, M. 1965 Acta Met. **13**, 591.

McMEEKING, R.M. 1977 J. Mech. Phys. Solids **25**, 357.

OATES, G. 1969 J. Iron Steel Inst. **207**, 264.

ODETTE, G.R. and LUCAS, G.E. 1983 J. Nucl. Matls. **117**, 264.

OSTERGREN, W.J. 1969 M.Sc. thesis, Brown University, Providence, R.I.

RICE, J.R. 1968 J. Appl. Mech. **35**, 379.

RICE, J.R. and JOHNSON, M.A. 1970 Inelastic Behavior of Solids (eds. Kanninen, M.F. et al.), p. 641, McGraw-Hill, N.Y.

RICE, J.R. and ROSENGREN, G.F. 1968 J. Mech. Phys. Solids **16**, 1.

RITCHIE, R.O., KNOTT, J.F. and RICE, J.R. 1973 Ibid. **21**, 395.

RITCHIE, R.O., SERVER, W.L. and WULLAERT, R.A. 1979 Metall. Trans. A **10A**, 1557.

ROSENFIELD, A.R., SHETTY, D.K. and SKIDMORE, A.J. 1983 Ibid. **14A**, 1934.

SHIH, C.F. 1983 Brown University Report No. MRL E-147, Providence, R.I.

SMITH, E. 1966 Proc. Conf. Physical Basis of Yield and Fracture, p. 36, Inst. Phys. and Phys. Soc., Oxford.

SUMPTER, J.D.G. and TURNER, C.E. 1976 Cracks and Fracture, ASTM STP 601, p. 3, ASTM, Philadelphia.

TRACEY, D.M. 1976 J. Eng. Matls. Tech. **98**, 146.

WALLIN, K., SAARIO, T. and TÖRRÖNEN, K. 1984 Met. Sci. **18**, 13.

WEIBULL, W. 1939 Ing. Vetenskap. Akad. Handl. **12**, 153.

WILLIAMS, M.L. 1957 J. Appl. Mech. **24**, 109.

WILSHAW, T.R., RAU, C.A. and TETELMAN, A.S. 1968 Engng. Fracture Mech. **1**, 191.

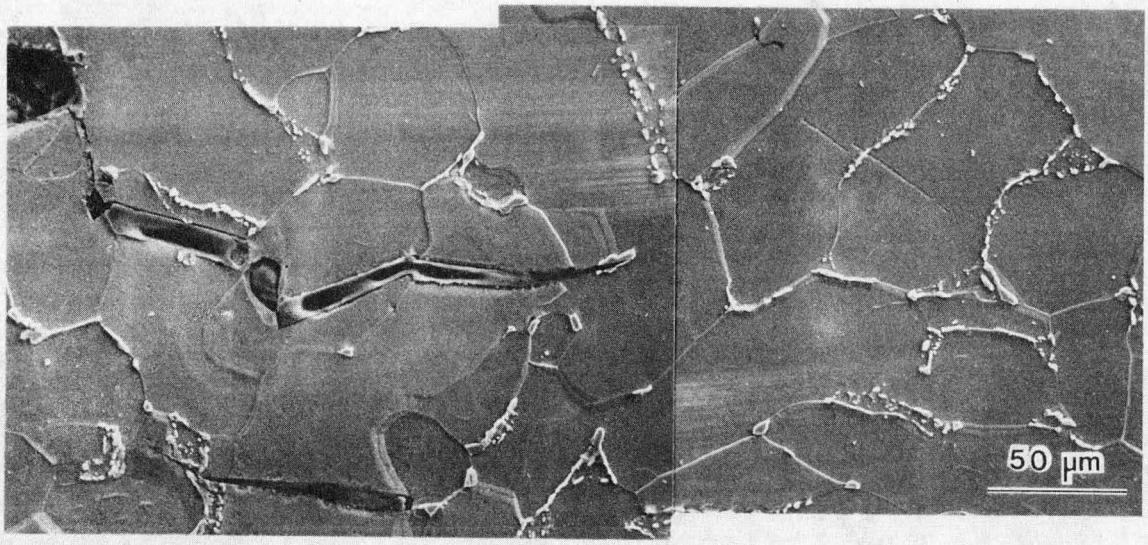

XBB 840-9415

Fig. 1: Transgranular cleavage cracks in a mild steel associated with cracked grain boundary carbides ahead of the main crack tip.

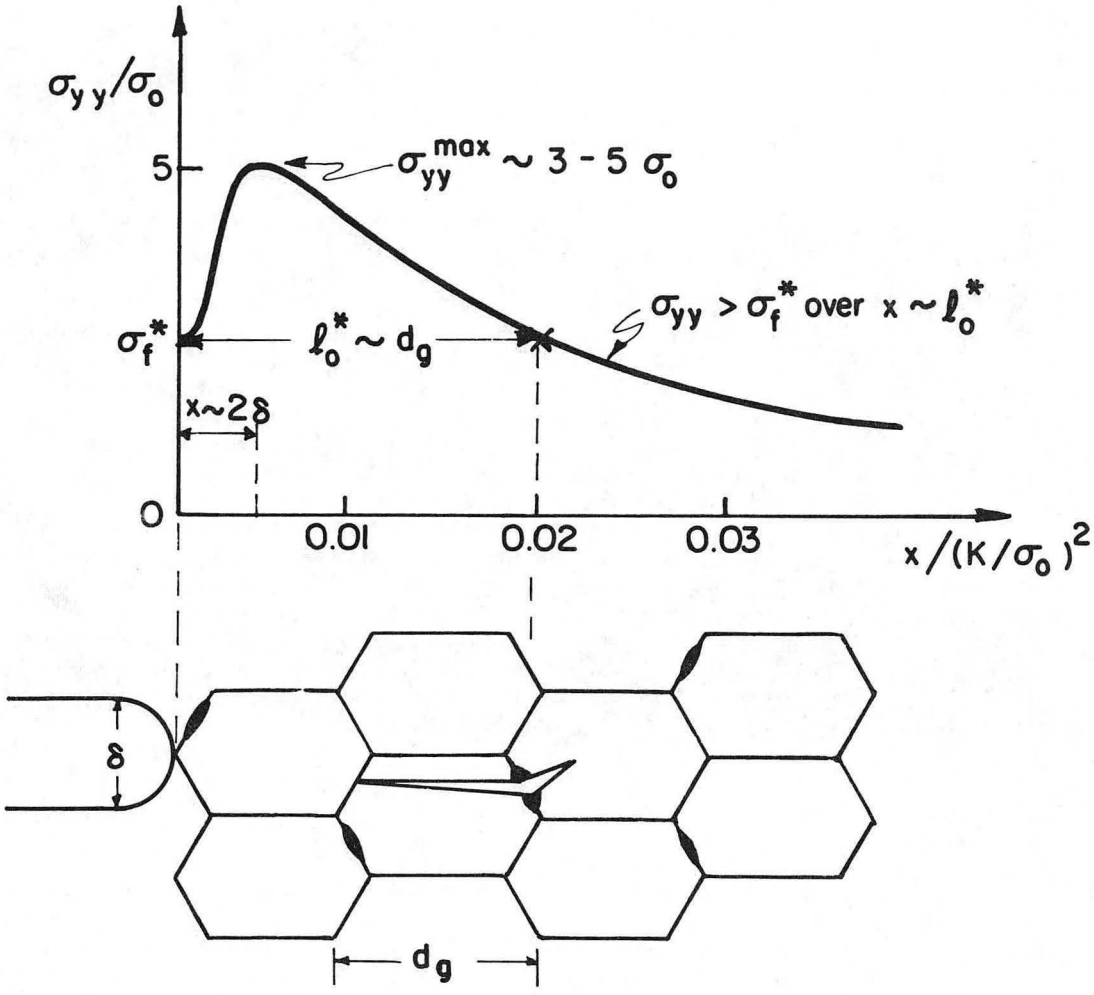

XBL 838-6216(a)

Fig. 2: Schematic illustration of the Ritchie, Knott and Rice (RKR) model for critical stress-controlled cleavage fracture directly ahead of a sharp crack.

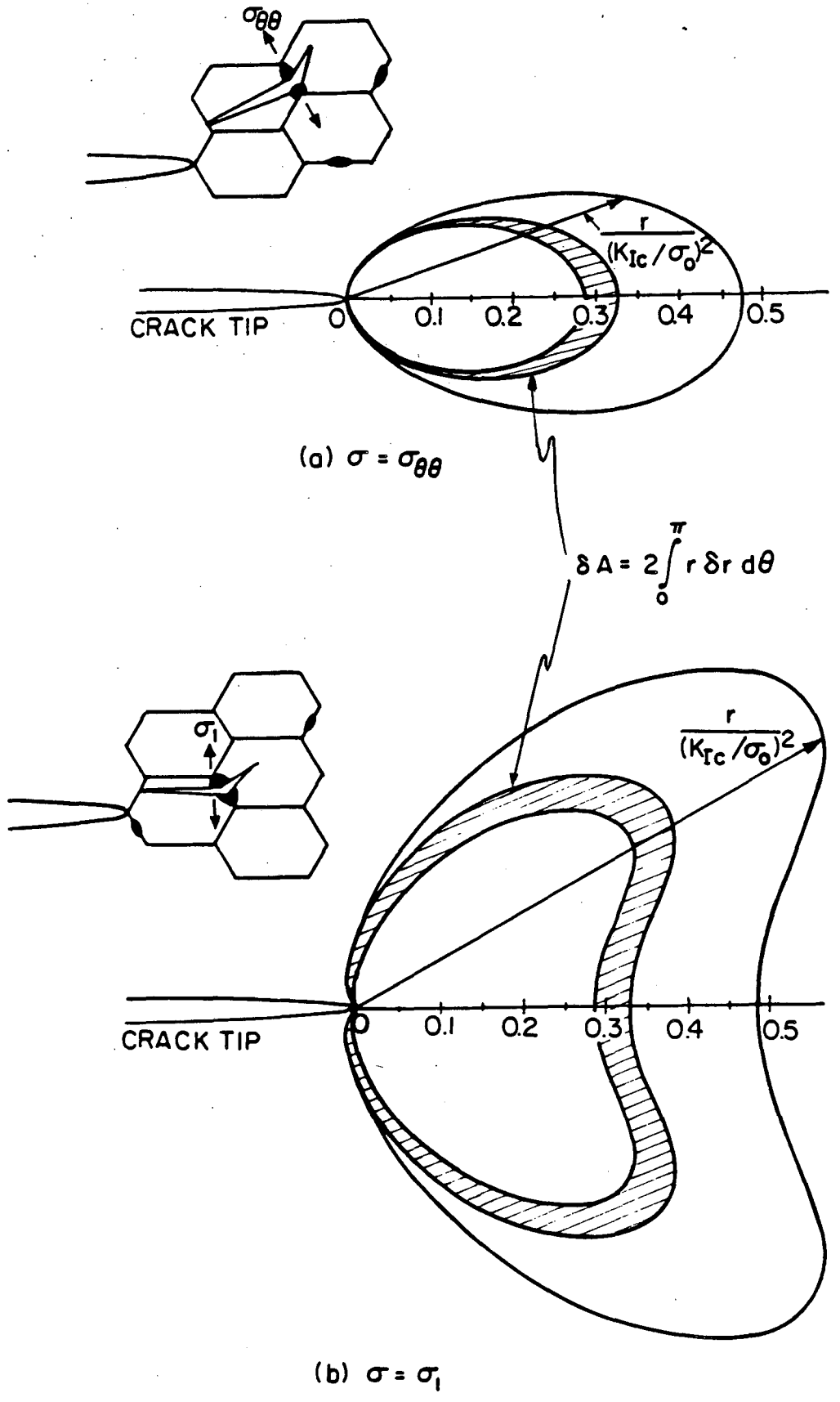

XBL 851-5801A

Fig. 3: Definition of the active zone, representing the region ahead of the crack tip where either a) the local tangential stress $\sigma_{\Theta\Theta}$ or b) the maximum principal stress σ_1 exceeds the particle fracture strength S.

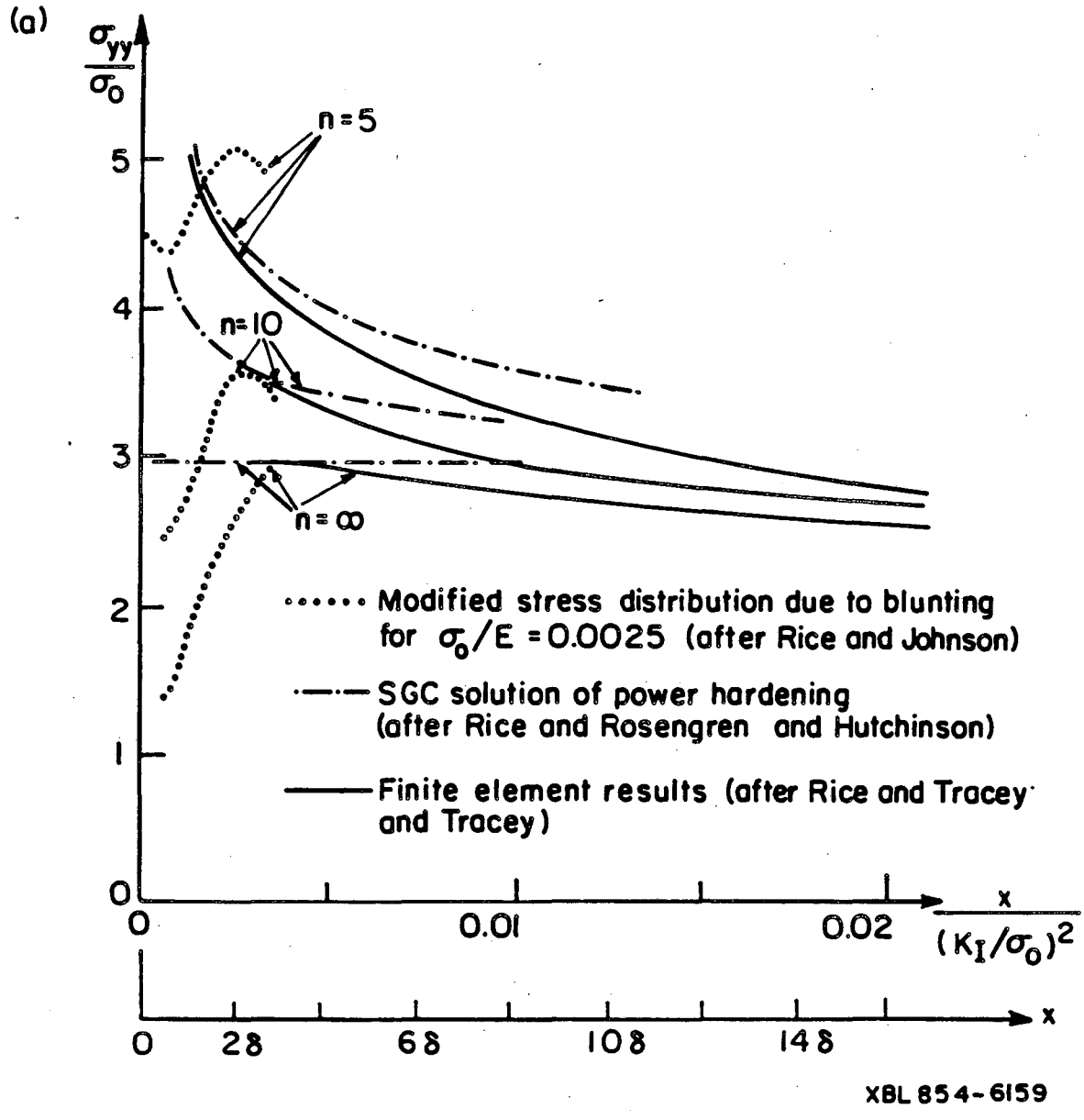

Fig. 4: Distribution of local tensile stress σ_{yy} as a function of distance x directly ahead of a tensile-loaded crack in plane strain. Shown are a) a comparison of the near-tip asymptotic HRR singular solution with numerical results for power law hardening (solutions are truncated very close to the tip by the Rice and Johnson blunting solution for σ_0/E = 0.0025), and b) a comparison of the far-field asymptotic linear elastic singular solution with numerical results based on ideal plasticity and power law hardening.

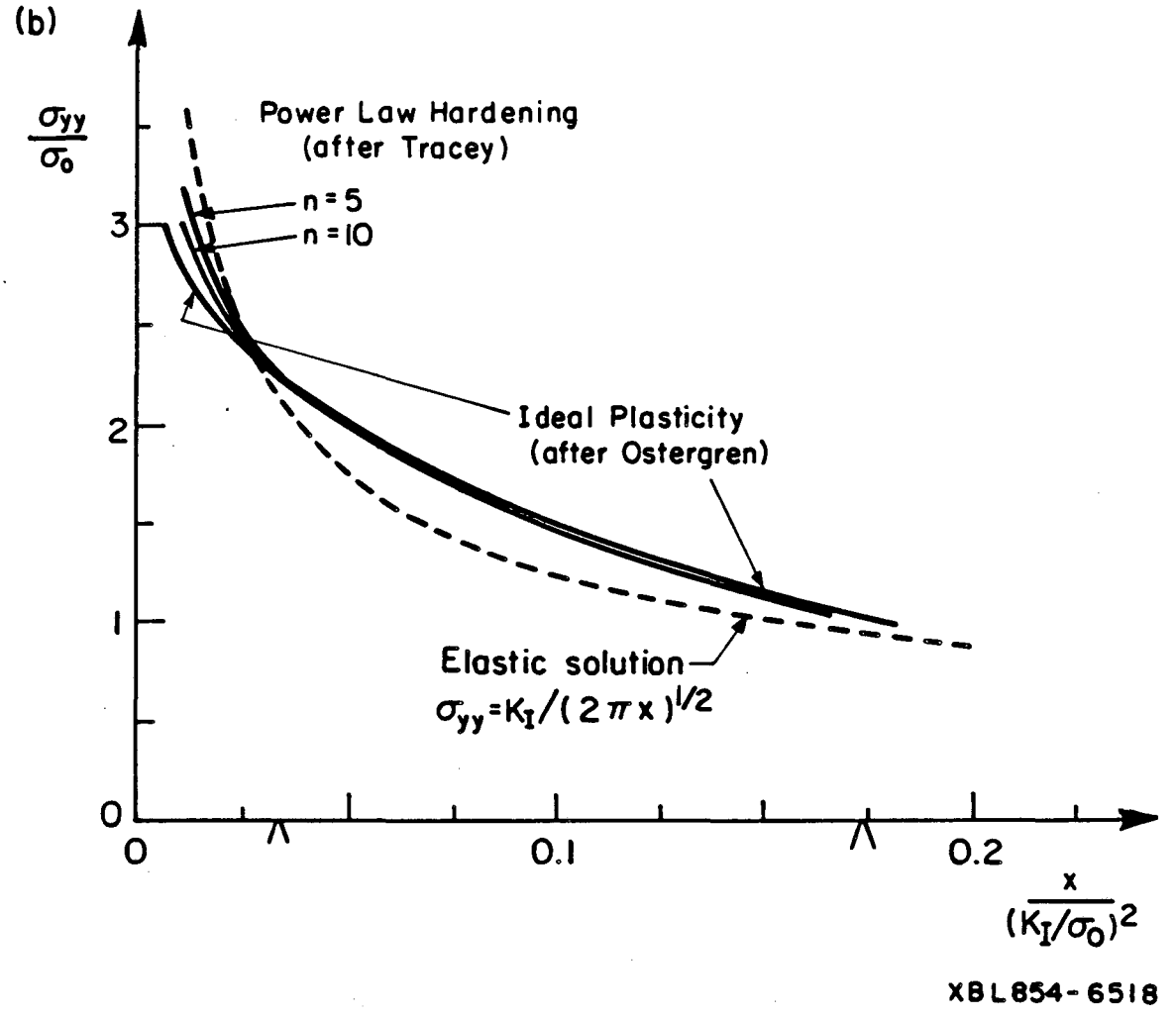
(b)
$\frac{\sigma_{yy}}{\sigma_0}$
Power Law Hardening
(after Tracey)
n = 5
n = 10
Ideal Plasticity
(after Ostergren)
Elastic solution
$\sigma_{yy} = K_I/(2\pi x)^{1/2}$
3
2
1
0
0
0.1
0.2
$\frac{x}{(K_I/\sigma_0)^2}$
XBL854-6518

Fig. 4(b)

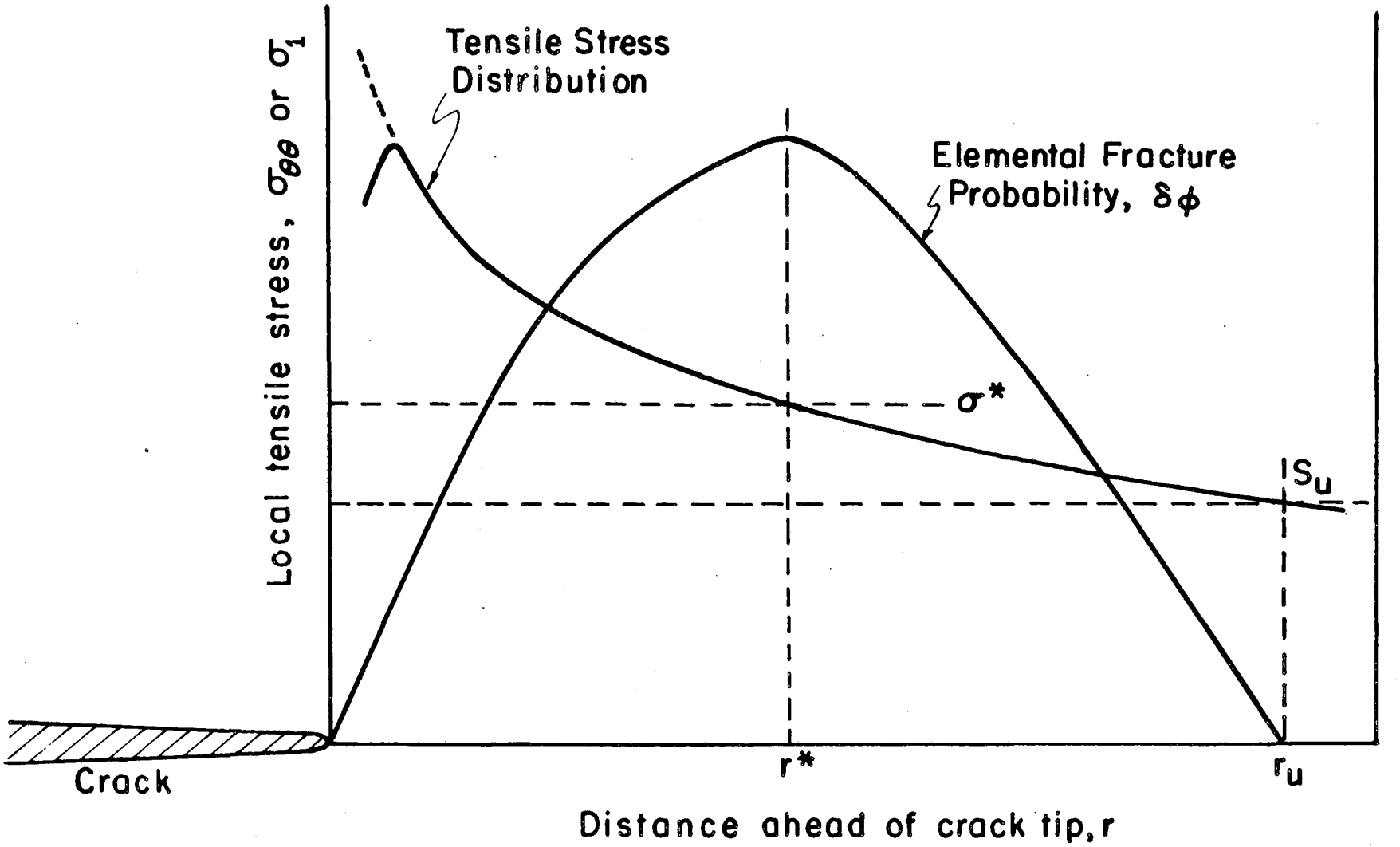

Fig. 5: Significance of the characteristic distance r^* and fracture stress σ^*, defined at the radial distance from the crack tip where the initial cracking event is most probable.

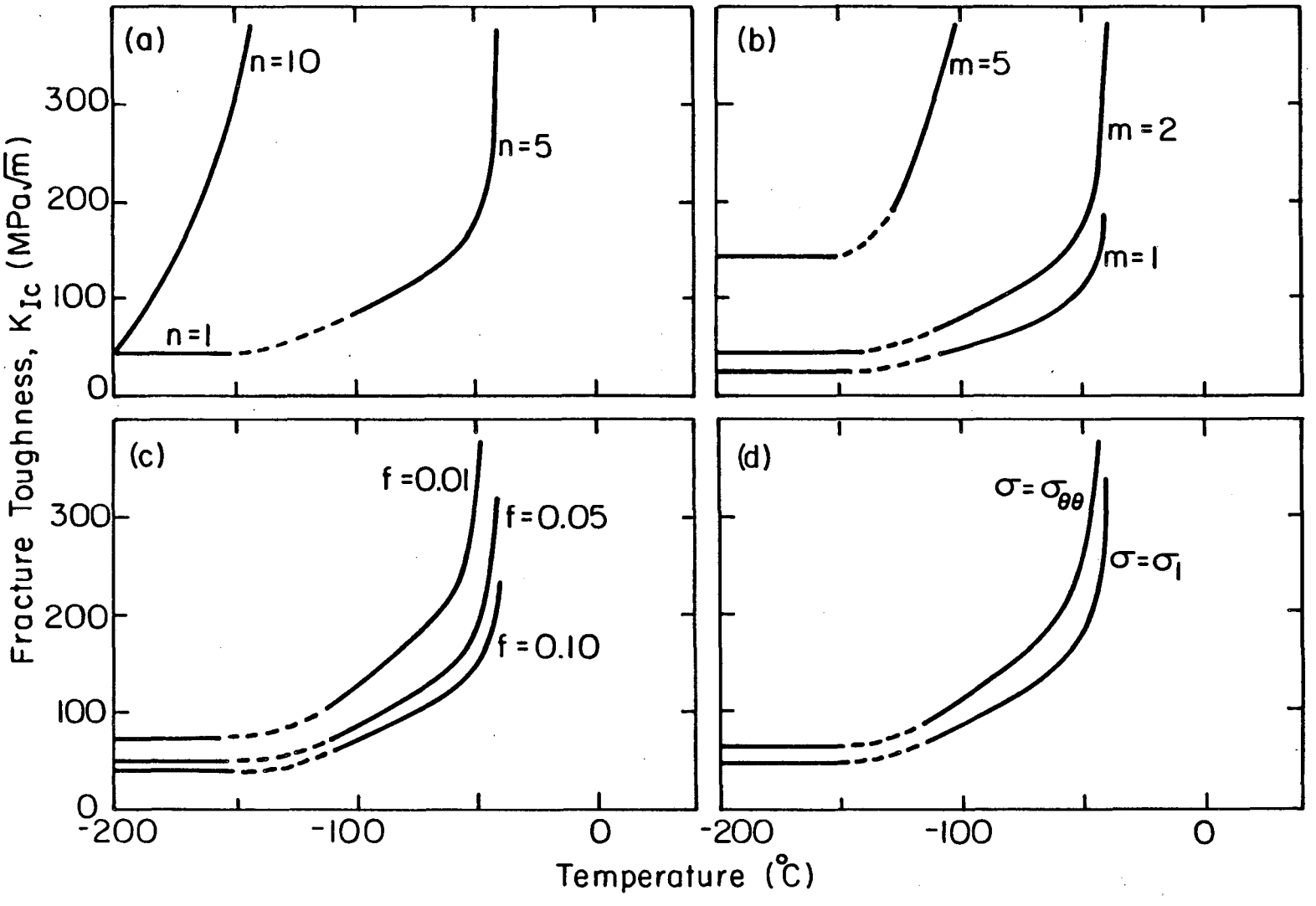

XBL 855-6282

Fig. 6: Predicted variation in fracture toughness, K_{Ic}, with temperature from lower shelf to ductile/brittle transition (Eqs. (15) and (19)), showing influence of varying a) work hardening exponents from n = 1 to 10, b) carbide size distribution from m = 1 to 5, c) fraction of eligible particles from f = 0.01 to 0.10, and d) relevant local stress, σ_1 or $\sigma_{\theta\theta}$. (Strength and microstructure data from AISI 1008 steel.)

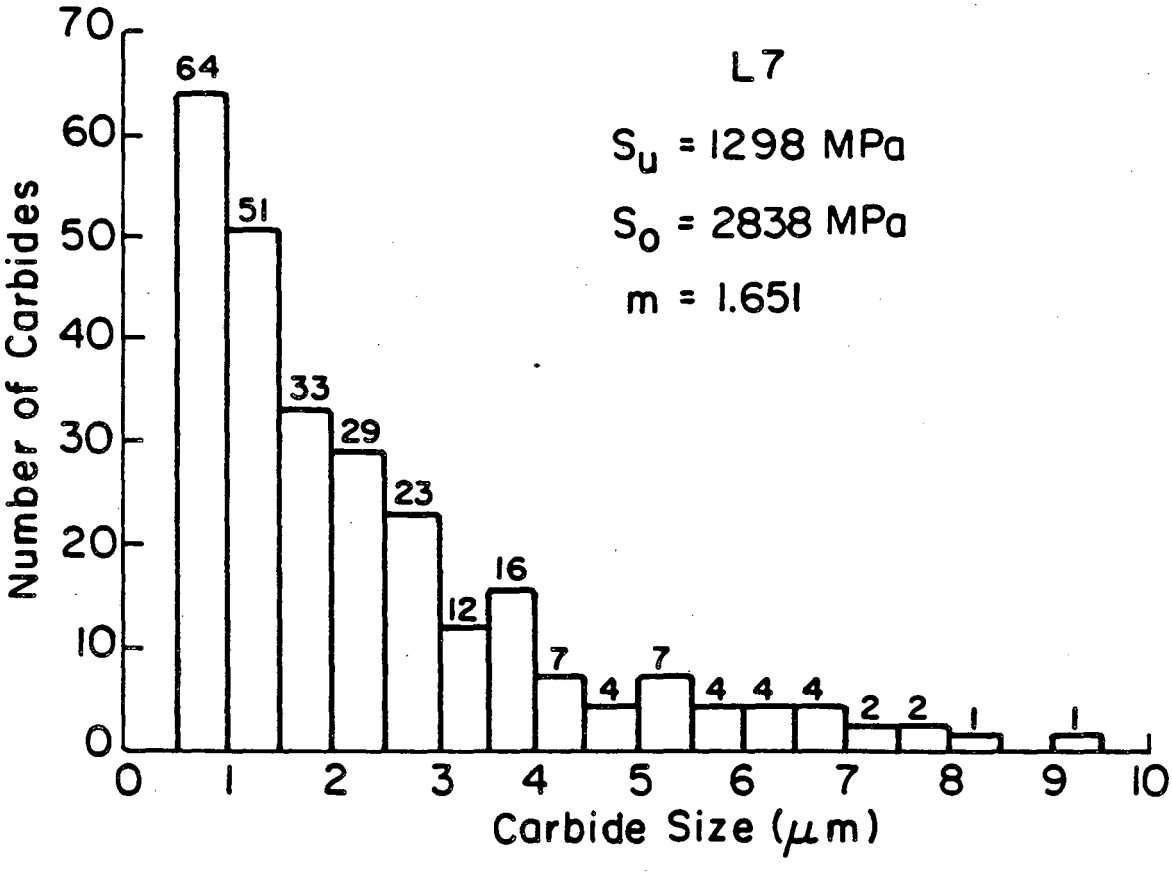

XBL 854-6157

Fig. 7: Size distribution of carbides, measured with an image analyzer in AISI 1008 mild steel after spheroidizing 7 days at 700°C (L7 microstructure).

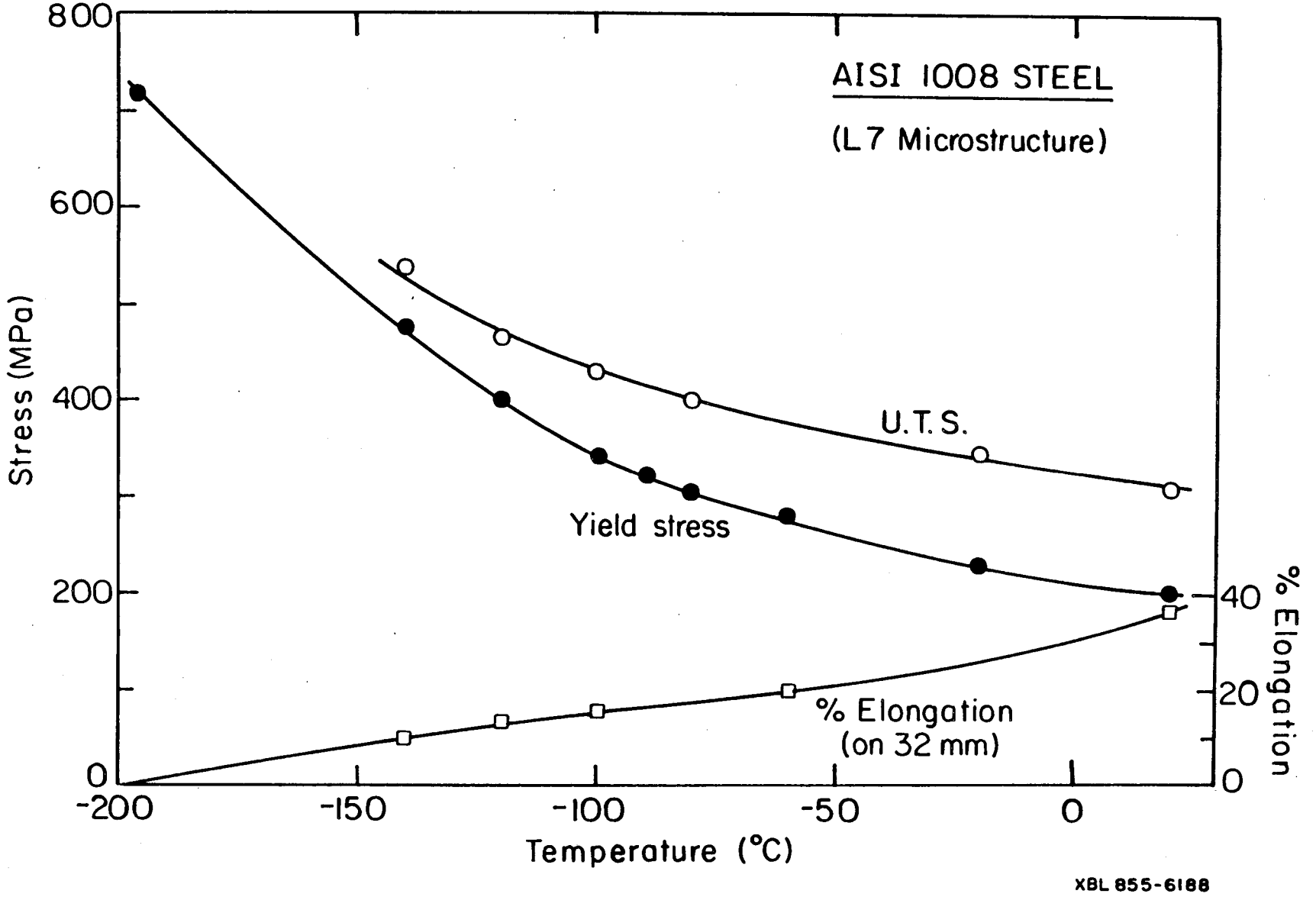

Fig. 8: Experimental measurement of the temperature dependence of uniaxial tensile properties in AISI 1008 mild steel. Shown are the (lower) yield stress, U.T.S. and % elongation (on 32 mm gauge length).

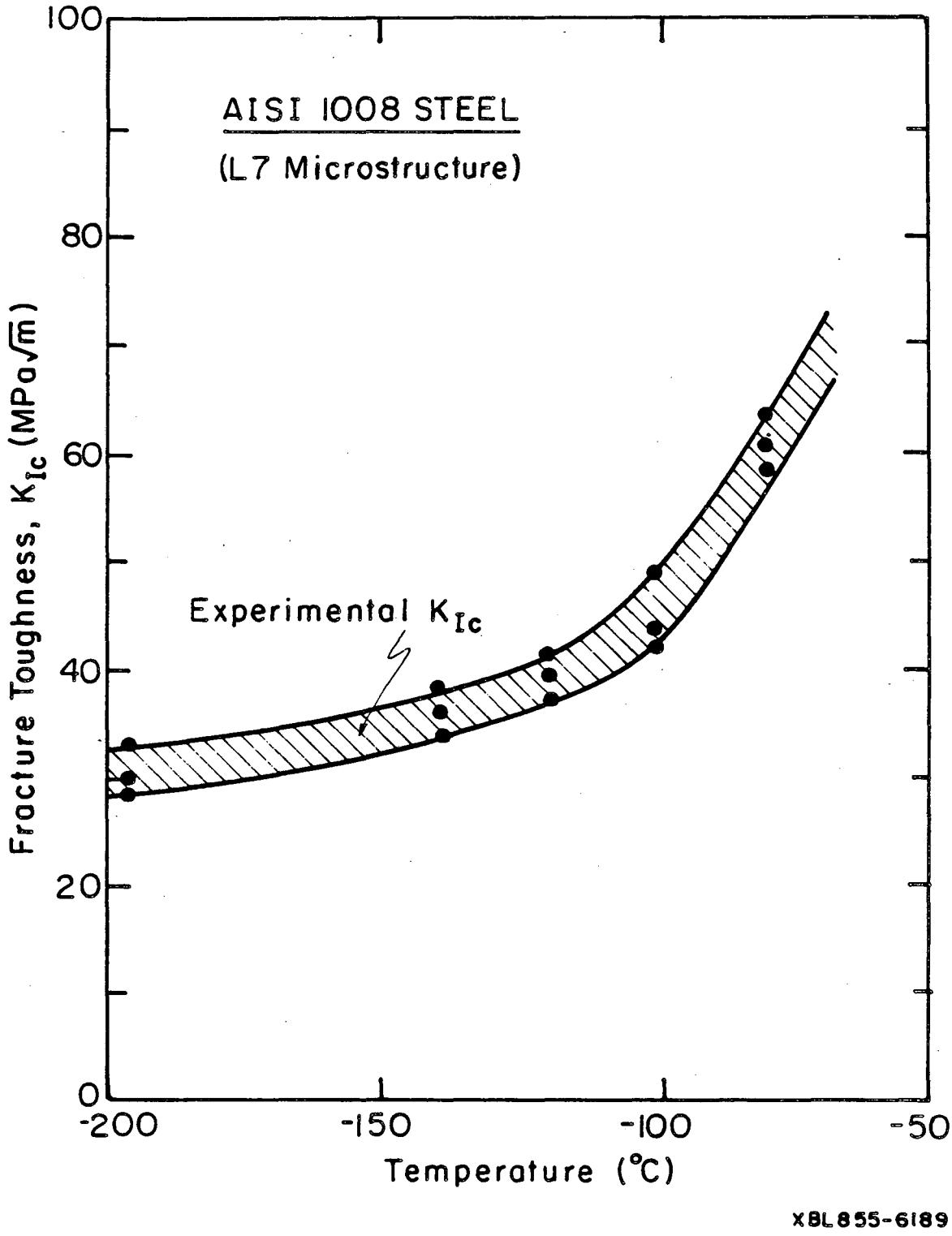

Fig. 9: Experimental measurement of the temperature dependence of plane strain fracture toughness K_{Ic} in AISI 1008 mild steel, based on four-point bend tests. Results above -100°C were computed from nonlinear elastic J_{Ic} measurements.

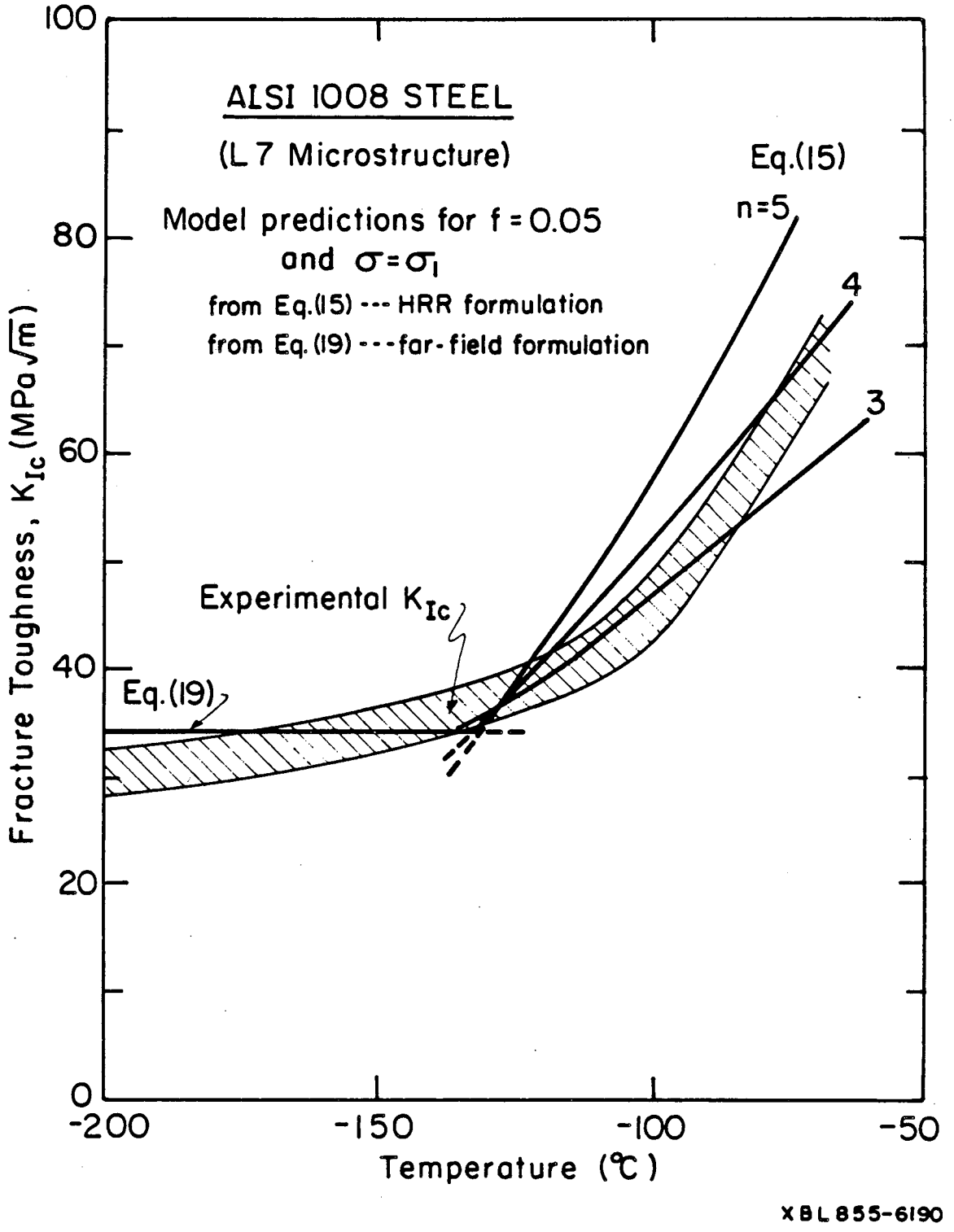

Fig. 10: Model predictions for mild steel, from Eqs. (15) and (19), for the temperature dependence of K_{Ic}, compared to experimental data in Fig. 9. Predictions are shown for work hardening exponents between 3 and 5.

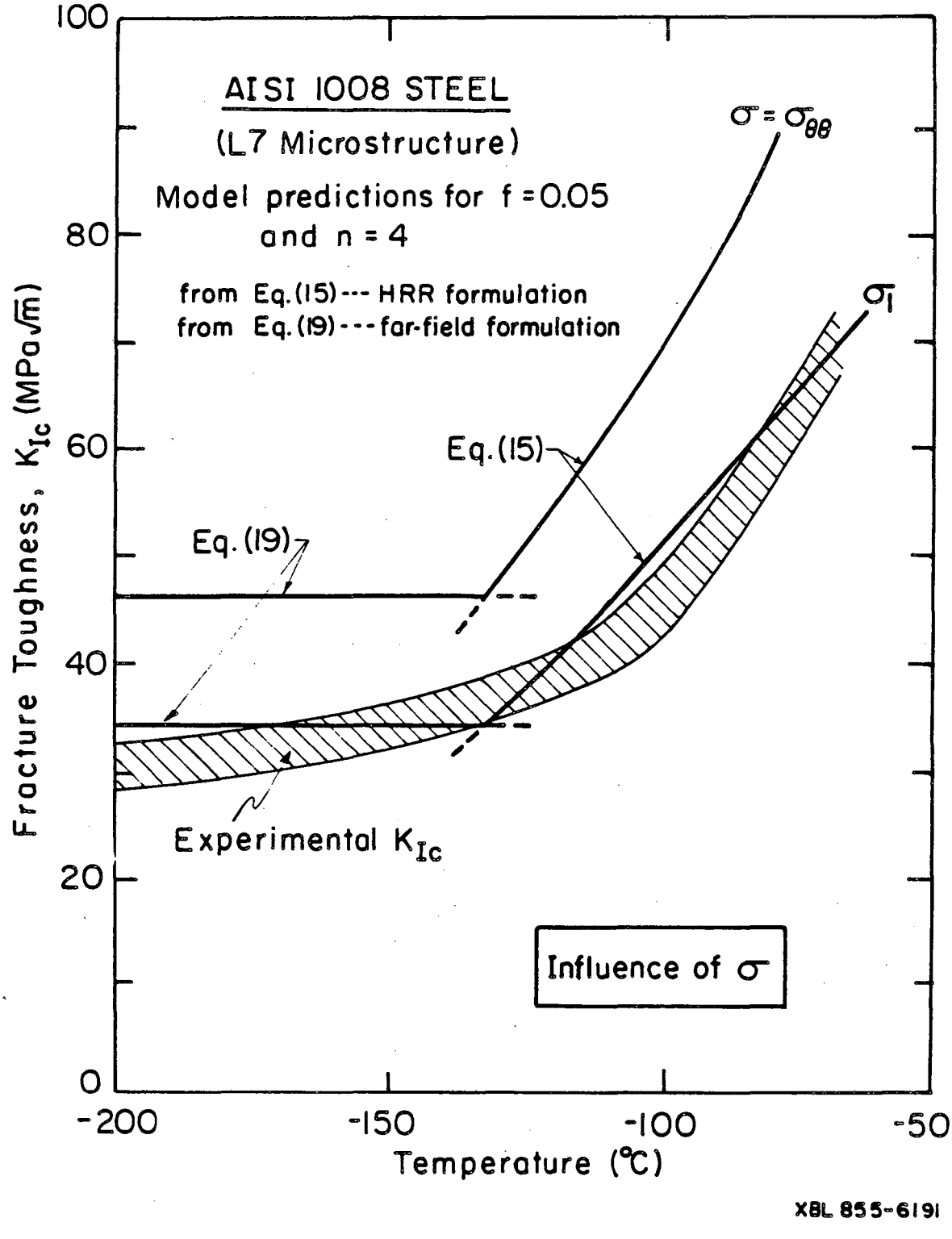

Fig. 11: K_{Ic} predictions for mild steel from Eqs. (15) and (19): effect of utilizing tangential stress $\sigma_{\theta\theta}$ model rather than model based on the maximum principal stress σ_1. Note how predictions based on $\sigma_{\theta\theta}$ overestimate the toughness.

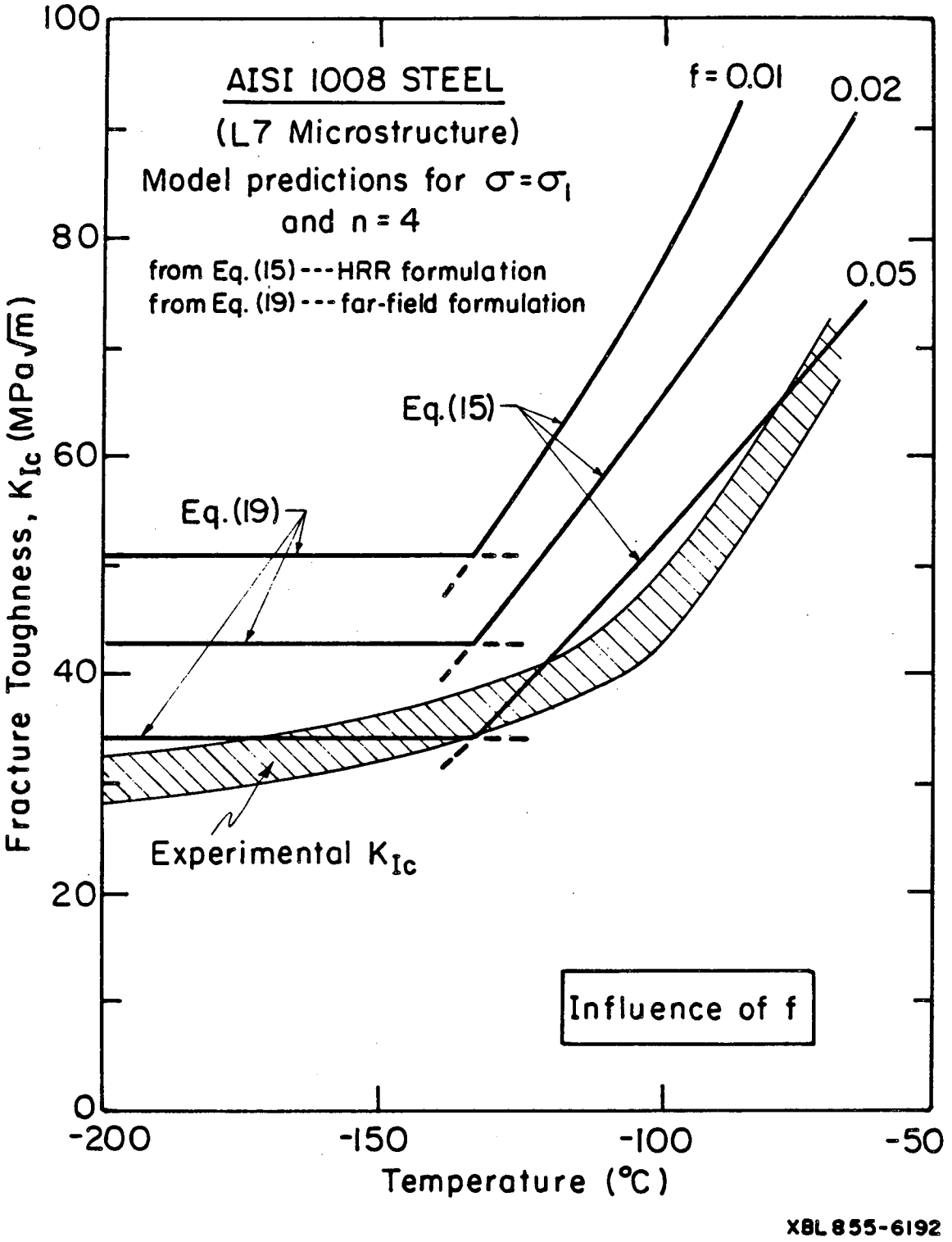

Fig. 12: K_{Ic} predictions for mild steel from Eqs. (15) and (19): effect of different values of f, representing the fraction of eligible particles **actively** involved in the fracture process.

LAWRENCE BERKELEY LABORATORY
TECHNICAL INFORMATION DEPARTMENT
UNIVERSITY OF CALIFORNIA
BERKELEY, CALIFORNIA 94720